



Assessing the impacts of simulated Ocean Alkalinity Enhancement on viability and growth of near-shore species of phytoplankton

Jessica L. Oberlander¹, Mackenzie E. Burke¹, Cat A. London¹, Hugh L. MacIntyre¹

¹Department of Oceanography, Dalhousie University, Halifax, Nova Scotia, N3H 4R2, Canada

5 Correspondence to: Jessica L. Oberlander (Jessica.Oberlander@dal.ca)

Abstract. Over the past 250 years, atmospheric CO₂ concentrations have risen steadily from 277 ppm to 405 ppm, driving global climate change. In response, new technologies are being developed to reduce emissions and to remove carbon from the atmosphere using negative emission technologies (NETs). One proposed NET is Ocean Alkalinity Enhancement (OAE), which would mimic the ocean's natural weathering processes, raising alkalinity and pH and sequestering carbon dioxide from the atmosphere. The potential impacts of OAE were assessed through an analysis of prior studies investigating the effects of elevated pH on phytoplankton growth rates and by experimental assessment of the pH-dependence of viability and growth rates in two near-shore isolates of phytoplankton. Viability was assessed with a modified Serial Dilution Culture – Most Probable Number assay. Chlorophyll a fluorescence was used to test for changes in photosynthetic competence and apparent growth rates. There were no significant impacts on the viability or growth rates of the diatom *Thalassiosira pseudonana* and the prymnesiophyte *Diacronema lutheri* (formerly *Pavlova lutheri*) with short-term (10-minute) exposure to elevated pH. However, there was a significant decrease in growth rates with long-term (days) exposure to elevated pH. Short-term exposure is anticipated to more closely mirror the natural systems in which OAE will be implemented because of system flushing and dilution. These preliminary findings suggest that there will be little to no impact on a variety of taxonomic groups of phytoplankton when OAE occurs in naturally flushed systems.

20



1 Introduction

The oceans cover about 70% of the planet's total surface area, support a vast number of organisms in varied environments, and have a pivotal role in climate regulation by storing heat and atmospheric gases (Galland et al., 2012). However, their ability to act as a carbon sink and buffer the changes occurring in the atmosphere is being pushed to its limit and is quickly becoming overburdened by the excess CO₂ emitted into the atmosphere (Galland et al., 2012). The increased uptake of CO₂ is causing a shift in the ocean's chemical equilibrium, leading to a decrease in the overall pH and a reduction in the concentration of carbonate (Lenton et al., 2018).

Negative Emission Technologies (NETs) are being developed to combat rising atmospheric concentrations of CO₂ and sequestering it for long timescales. Ocean Alkalinity Enhancement (OAE) is one promising NET that would enhance the ocean's natural weathering processes while also restoring the oceanic pH and carbonate system to their natural state. The ocean has already absorbed c. 40% of anthropogenic emissions from the atmosphere (Renforth & Henderson, 2017), and the addition of alkalinity from OAE would increase this. The additional carbon would be stored in the form of bicarbonate (HCO₃⁻), which has a residence time of c. 1,000 years in the ocean. Implementation of OAE at large scale would like be through addition of hydroxide (OH⁻) to surface coastal oceans. The increased alkalinity, would react with CO₂ in the surface ocean to form bicarbonate, leading to CO₂ invasion from the atmosphere to compensate for the drawdown. Alkalization and the subsequent reaction between OH⁻ and CO₂ would lead to changes in surface pH and might alter which carbon species dominates. The changes might have negative impacts on marine biota, notably phytoplankton as their growth depends on uptake and assimilation of CO₂.

The implementation of OAE will almost certainly need to be land-based, as the release of human-made matter into the open ocean is currently prohibited under the *Convention on the Prevention of Marine Pollution by Dumping of Wastes and Other Matter, 1972*, better known as the London Convention. This means any addition of alkalinity will need to happen along the coast, likely at a previously established outflow or waste pipe, to remain in compliance with the Convention. Before any large-scale implementation can begin, it must be confirmed that there are no negative impacts on marine biota, especially phytoplankton as they are the base of the majority of marine food webs and play a significant role in biogeochemical cycling in the ocean (Winder and Sommer, 2012).

All phytoplankton rely on ribulose-1,5,-biphosphate carboxylase/oxygenase (Rubisco) in the Calvin cycle to assimilate CO₂ (Raven et al., 2017). The reaction is generally undersaturated in regards to CO₂ since the current concentration of CO₂ available for phytoplankton (*i.e.*, dissolved in the ocean) is only about 10 mmol m⁻³ (Raven et al., 2017) while Rubisco's half-saturation concentration is 105 – 290 mmol m⁻³ (Jordan & Ogren, 1981; Tcherkez et al., 2006; Badger & Bek, 2008; Shih et al., 2016).



The low concentration of available CO₂ reflects the dominance of the dissolved inorganic carbon (DIC) system by HCO₃⁻ at pH 6 – 9.

55

As phototrophs, the cellular requirement for CO₂ remains high in phytoplankton and most have adapted to the limitation by acquisition of carbon concentrating mechanisms (CCMs). The CCMs facilitate uptake of CO₂ by its active transport across the cell membrane and/or by uptake of HCO₃⁻ through anion exchange, followed by its conversion to CO₂ by carbonic anhydrase (Colman et al., 2002; Nimer et al., 1997). Both the CCM and carbonic anhydrase are likely to be vulnerable to changes in pH, and thus OAE, as they rely on a pH gradient to function. Further, not all species can actively transport HCO₃⁻ into the cell or have carbonic anhydrase; thus, there is a potential for selective disruption of the community and an increase in the metabolic costs of CCM use. These potential changes could lead to an overall reduction in community growth rates or to taxonomic shifts within the assemblage in response to alkalization.

60

65

Previous research has documented a clear relationship between phytoplankton growth rates and pH, with deviations from the norm in either direction resulting in negative impacts (Hansen, 2002). There are certain species of phytoplankton, notably the diatom *Phaeodactylum tricornerutum*, that are able to tolerate a pH above nine and below seven without reducing their growth rate to zero (Berge et al., 2010; Hansen, 2002). A decrease in growth rate could be due to a change in vitality (*i.e.*, reduced metabolic competence, *e.g.*, a reduction in photosynthetic efficiency), or because of a reduction in viability (*i.e.*, reproductive competence) in a fraction of the population. Quantifying possible impacts of OAE on phytoplankton – and higher trophic levels – is vital for evaluating its suitability as a NET.

70

75

This study addresses potential impacts of OAE on phytoplankton in two ways. First, published data were collated and analysed to quantify the effect of elevated pH on the growth rates of a range of cultured phytoplankton. Second, the viability, growth rates, and photosynthetic competence (as F_v/F_m) was examined for cultures of *Thalassiosira pseudonana* Clone CCMP 1335 and *Pavlova lutheri* Clone CCMP 1325 exposed to both short- and long-term elevated pH and alkalinity in cultures with gas exchange.

2 A review of the pH-dependence of growth rates

2.1 Literature Review & Data Digitization

80

A literature review was conducted to collate data from various studies that have used either batch or semi-continuous cultures to assess the effect of elevated pH on growth rates of phytoplankton. Criteria for the use of an article in this review included species/strains of phytoplankton indicative of marine systems, elevated pH, and the inclusion of growth media, irradiances, and temperature in the methods. The majority of the studies analysed were by Hansen and colleagues, to ensure consistent



approaches were used. Their protocols controlled nutrient stoichiometry to ensure DIC limitation of growth and most were in
85 batch cultures without ventilation to replenish CO₂. A summary is given in Supplementary Table 1.

The data from each study was digitized using OriginPro 2022b (9.9.5.167, Learning Edition) to test for the relationship between
growth rate and pH. The data were either growth curves (variations in cell concentration over time, from which growth rate
can be estimated) or growth rates and parallel variations in pH. To determine error associated with the digitization, random
90 numbers were generated and plotted against a linear series and the plot was then digitized the same way. The root mean square
error (RMSE) of the y-axis values in the randomly generated plot was 0.4% of the maximum of the data range.

2.2 Model Fitting

For articles that listed cell concentrations, these were ln-transformed and fit against time using Equation 1. This is a
modification of the model used by Bannister (1979) to describe the photosynthesis-irradiance response curve, recast to include
95 a non-zero intercept. The choice of Bannister's formulation over other commonly used growth models (Zwietering et al., 1990)
was based on its flexibility in accommodating abrupt versus gradual transitions between the exponential and stationary phases
of the response (Jones et al., 2014).

$$\ln[cells_t] = (\ln[cells_{fin}] - \ln[cells_{init}]) \cdot \frac{day}{((t_{stat})^b + t^b)^{\frac{1}{b}}} + \ln[cells_{init}], \quad (1)$$

where t is time (d) and t_{stat} is the time to stationary phase; $cells_{init}$, $cells_{fin}$, and $cells_t$ are cell concentrations (cells mL⁻¹) at $t = 0$,
100 in stationary phase, and at time t ; and b (dimensionless) is a parameter that defines the curvature in the function as the growth
rate declines in the transition between exponential and stationary phase.

The maximum and time-dependent growth rates, μ_m and μ (d⁻¹), were then determined empirically from the fit to Equation 1
as tangents to the growth curve calculated in increments of 0.014 d. The growth rate was expressed in dimensionless terms as
105 μ/μ_m for comparison between studies. These relative growth rates were calculated at times when corresponding pH data were
collected and the resulting curve was fitted with either a biphasic (Equation 2a & b) or 1st-order kinetic model (Equation 2a &
c) that describes the decline in growth rate above a threshold pH value (modified from MacIntyre et al., 2018);

$$\frac{\mu}{\mu_m} = 1 \text{ for } pH \leq pH_{Th}, \quad (2a)$$

and

$$110 \frac{\mu}{\mu_m} = (1 - \alpha) \cdot \exp(-k_1(pH - pH_{Th})) + \alpha \cdot \exp(-k_2(pH - pH_{Th})) \text{ for } pH > pH_{Th}, \quad (2b)$$

or

$$\frac{\mu}{\mu_m} = \exp(-k \cdot (pH - pH_{Th})) \text{ for } pH > pH_{Th}, \quad (2c)$$



115 where α (dimensionless) is a coefficient that partitions the biphasic response and varies between 0 and 1, k_1 and k_2 and k (pH^{-1}) are sensitivity coefficients that relate to the slopes; and pH_{Th} is the threshold pH above which growth rates decline with pH. The threshold model of pH change is utilized here as it is a common model that allows “shouldering” in various studies of inactivation (Hijnen, 2006; Weavers & Wickramanayake, 2001). Although the focus of these studies is UVC photoinactivation rather than pH limitation, the mechanistic underpinning of progressive debilitation, often with “tailing” (i.e., a biphasic response) is supported by observations of “shouldering” in the data followed by progressive debilitation in both scenarios.

120

For those studies that reported growth rates rather than cell concentrations, the fitting with Equation 1 was omitted, and the digitized data were fit only with Equation 2. The choice of the biphasic or 1st-order model was based on the values of k_1 and k_2 in the biphasic model. If the means differed by less than the sum of the standard errors of the estimates, the 1st-order model was used; otherwise, the biphasic model was. Data sets that could not be fit with the models because there were fewer data points than fit parameters or because no pH threshold was defined were omitted from subsequent analysis.

125

The model fits were used to generate a pH-dependent growth curve in increments of 0.005 pH units to define the pH values at which there was a 10% and 90% reduction in growth rate. Primer 7 software (PRIMER-e v7.0.21) was used to test for differences in taxonomic groups in Figure 1 using analysis of similarity (ANOSIM).

130 **2.3 Comparison of threshold response between taxonomic groups**

The normalized growth curves for all species are shown in Figure 1a. The threshold pH and pH values at which there was a 10% and a 90% reduction in growth rate are compared in Figure 1b. The data were grouped by taxonomic status – divisions, except the classes containing raphidophytes and diatoms with the Heterokontophyta – and compared by ANOSIM. There are statistically significant difference between groups ($p = 0.001$), with the major differences being between dinoflagellates and all other groups except for prymnesiophytes, and between cryptophytes and diatoms (Table 1). A similarity percentage analysis (SIMPER) shows that the factor driving this difference is the pH at which μ was reduced by 90% in most cases, indicative of taxonomic differences in response to extreme alkalization. In some comparisons with dinoflagellates, the difference is more evenly distributed between the three pH factors, indicating higher sensitivity of the dinoflagellates at lower levels of alkalization.

140



145 *Table 1:* R significance level (ANSOIM) for differences between taxonomic groups in Figure 1c and d. Variables include the threshold pH, pH for a 10% reduction in growth rate, and pH for a 90% reduction in growth rate. Significant difference are indicated by asterisks.

	Cryptophyte	Prymnesiophyte	Chlorophyte	Raphidophyte	Diatom	Dinoflagellate
Cryptophyte						
Prymnesiophyte	0.2					
Chlorophyte	0.2	0.2				
Raphidophyte	1	0.33	0.25			
Diatom	0.0071*	1	0.1	0.14		
Dinoflagellate	0.001*	0.89	0.003*	0.019*	0.054*	

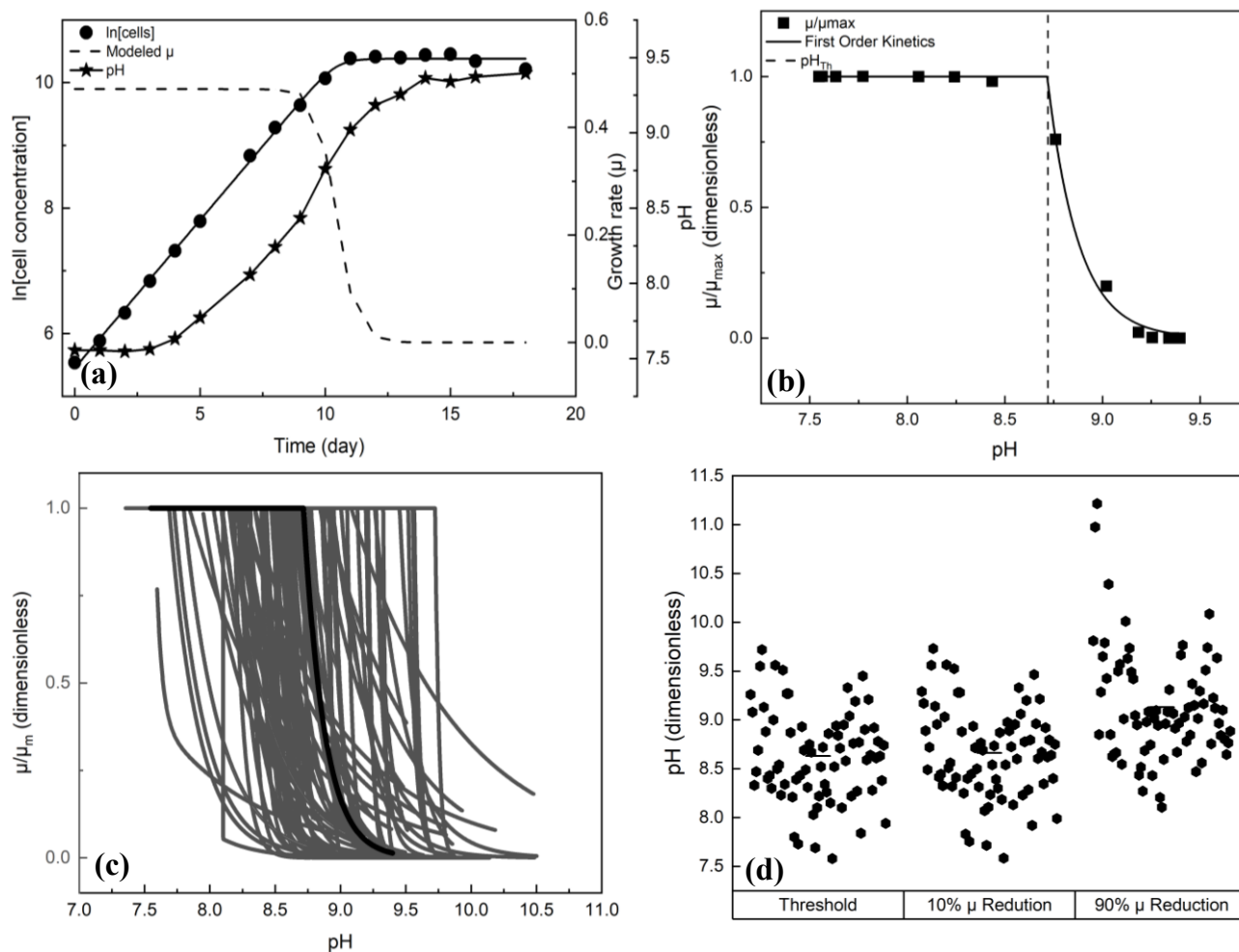


Figure 1: (a) Example of Bannister fit for *Heterocapsa triquetra*, NIES 7 (Berge et al., 2012), with the modeled growth rate and corresponding pH. (b) Example of the 1st-order kinetic model fit for *Heterocapsa triquetra*, NIES 7 (Berge et al., 2012), threshold pH 8.72 ± 0.005 . (c) Compilation of the 72 dimensionless relationships between relative growth rate and pH for the different species or environmental conditions. The black line represents the *Heterocapsa triquetra*, NIES 7 fit. See Supplement 1 for further information. (d) The calculated threshold pH, pH for a 10% reduction in growth rate, and pH for a 90% reduction in growth rate for the growth curves in (a). The black lines represent the median values.

For all of the species investigated (Figure 1), the median threshold pH is above 8.5, meaning about 50% of species would not be impacted by the anticipated maximum pH increase associated with OAE. The other 50% of species might be impacted.

150 The variability in response could be attributed to a number of different factors including the concentrations of DIC (Hansen et al., 2007; Söderberg & Hansen, 2007; Søgaard et al., 2011), light intensity (Söderberg & Hansen, 2007; Nielsen et al., 2007), or adaptative differences within species isolates. However, the effects of DIC and light intensity cannot be assessed



directly from these studies as only three of the thirteen reviewed report DIC availability, and only two included variations in light intensity in the experimental design.

155

These studies allowed a limited number of comparisons of growth rates between cultures maintained at constant, elevated pH in semi-continuous culture and those where the pH was allowed to drift in sealed batch cultures. A comparison of responses under these conditions is shown in Figure 2 for three dinoflagellates in the genus *Ceratium*. The average threshold pH in the constant-pH experiments is not statistically different than the drift experiments when results for *C. furca* and *C. fusus* in both conditions were grouped with the responses of *C. tripos* in pH-drift culture. In *C. tripos*, there was no detectable decrease in growth rate with pH in the semi-continuous cultures, although there was in the batch-drift cultures. As the absence of an effect could not be parameterized within the framework of the model, the semi-continuous culture is not presented in Figure 2.

160

165

In *C. furca* and *C. fusus*, the similarity of responses in the constant-pH and pH-drift cultures suggest that differences in other parameters between the culture methods (DIC, light, nutrients, etc.) have less effect on growth than changes in pH, and/or that there was no long-term acclimation to pH in the semi-continuous cultures. In contrast, there were significant differences in *C. tripos* between the conditions, with no observable effect of pH in the constant-pH culture. This might be because the difference is driven primarily by another factor, likely reduced DIC in the pH-drift experiment, or because the cells were able to acclimate to elevated pH after longer exposure. However, both experimental set-ups are a mismatch for the likely discharge of alkalinity into well-mixed waters where exposure time will be much shorter.

170

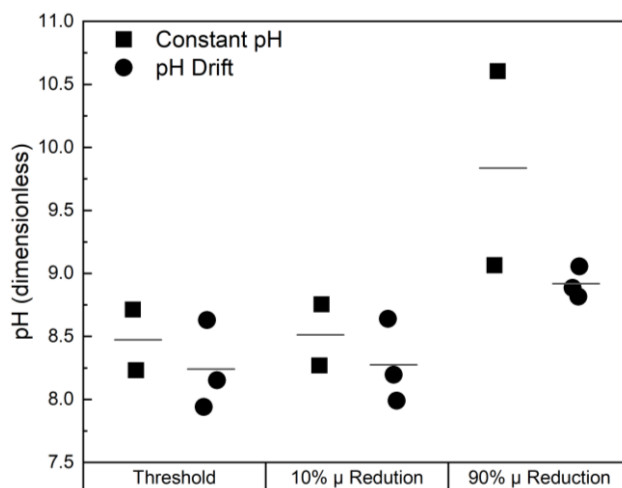


Figure 2: Comparison of the threshold pH above which there is reduction in growth rate (pH_{Th}), the pH for a 10% reduction in growth rates, and the pH for a 90% reduction in growth rates in *Ceratium furca*, *C. fusus*, and *C. tripos* that were maintained at a constant pH in semicontinuous culture or were kept in batch cultures in which the pH was allowed to drift. The black lines represent the mean values. There was no change in growth rate in *C. tripos* maintained at constant pH, although there was during the pH-drift experiment.

3 Examining the impact of prolonged, elevated pH on phytoplankton with and without DIC resupply

Most prior work investigating the impacts of elevated pH on phytoplankton growth did not permit for DIC resupply, which is necessary for OAE to function as a NET. The effect of this is illustrated in Figure 3a and 3b, in which batch cultures of the diatom *Thalassiosira pseudonana* Clone CCMP1335 were either aerated or not. (Details of the culture conditions and parameter estimates are given in Supplement 2). There are clear differences between the two cultures in pH, DIC, and a proxy for biomass. There were also clear differences in the descriptors of the diatom's abundance and physiological status.

In the sealed (pH drift) incubation, there was a progressive draw-down of DIC to about 50% of the initial value and a rise in pH to 9.26 ± 0.03 in stationary phase (Days 4-6; Figure 3a). Estimation of the partitioning of the carbonate system with CO2SYS (Lewis and Wallace, 1998) showed that the DIC pool was dominated by carbonate ($63 \pm 1\%$ of the DIC pool) and CO₂ concentrations were $<0.2 \mu\text{mol}^{-1}$ in this period. In contrast, the initial draw-down of DIC was reversed in the aerated culture when the culture entered stationary phase and CO₂ demand was reduced, returning to the initial value. The initial increase in pH was significantly reversed over the same period, and average 8.53 ± 0.05 over the last 3 days of stationary



phase (Days 6-8; Figure 3b). Based on CO₂SYN, the DIC pool was dominated by bicarbonate ($79 \pm 1\%$) and CO₂ concentrations were $>3.5 \mu\text{mol}^{-1}$ and rising during this period.

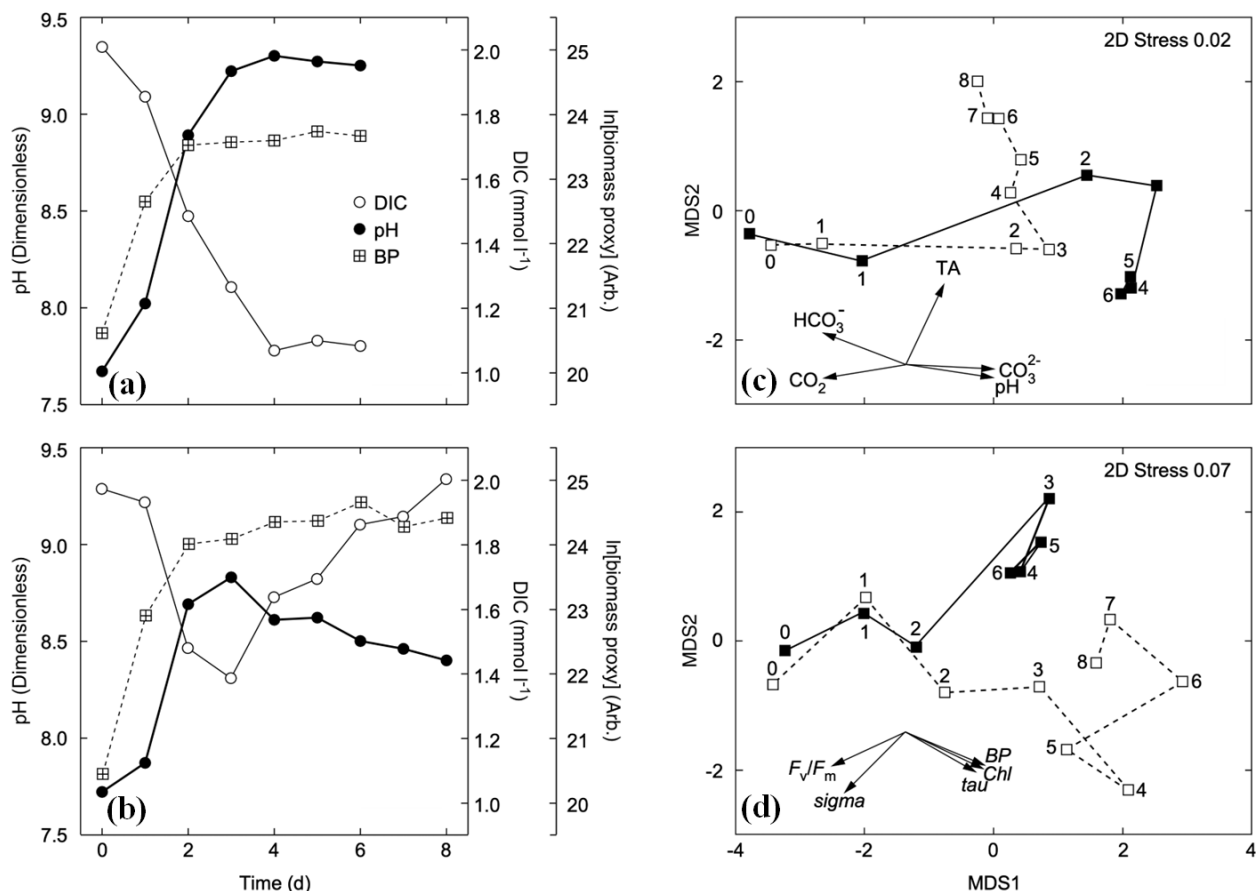


Figure 3: Changes in pH, DIC, and a proxy for biomass (BP) in cultures of the diatom *Thalassiosira pseudonana* that were sealed (a) or aerated (b) during growth (see Supplement 2 for details). Metric multidimensional scaling plots are of (c) carbonate system variables and (d) biotic variables describing phytoplankton abundance and physiological status. Data were normalized by variable prior to analysis. The resemblance measure between samples is Euclidian distance. Closed symbols are for the sealed culture; open symbols are for the aerated culture. Numbers by the symbols refer to time (d) from inoculation. Vectors are for the factor loadings on input variables in the ordination. Note the divergence of trajectories in both the abiotic and biotic variables following exponential-phase growth (Day 0-1).



190 There is clear separation between the aerated and pH-drift cultures following the period of exponential growth (Days 0-1) with respect to both the carbonate system parameters (Figure 3c) and biological parameters describing abundance and physiological status (3d). The variation in the biological parameters was compared to the abiotic parameters using BEST, an iterative test based on correlations between a matrix of pairwise similarity coefficients based on the biotic data, against similar matrices of all possible combinations of 1-5 abiotic parameters. The highest correlations were for combinations of 2-
195 4 variables (Spearman's R, 0.59 – 0.61) that included CO₂ and 1-3 other variables (see Supplement 2). These results suggest that the responses to OAE cannot necessarily be inferred from pH drift experiments.

4 Assessing the effects of short- and long-term alkalization on viability, growth, and photosynthetic competence in two coastal phytoplankton

4.1 Culturing Techniques

200 The phytoplankton cultures used for examining the impacts of simulated OAE on viability, growth rates, and photosynthetic competence were the diatom *Thalassiosira pseudonana*, Clone CCMP 1335, and the prymnesiophyte *Diacronema lutheri* (formerly *Pavlova lutheri*), Clone CCMP 1325, both of which were obtained from the National Center for Marine Algae and Microbiota (NCMA, East Boothbay, ME, USA). These were chosen as they are representative of taxa that dominate during the spring and fall blooms of near-shore, temperate waters. The phytoplankton were tested for reductions in relative viability
205 (RV), photosynthetic competence (as the proportion of functional photosystem (PSII) reaction centres), and growth rate (μ), following both chronic (days) and transient (10-minute) exposure to sodium hydroxide (NaOH).

The cultures were maintained in balanced growth in semi-continuous culture (MacIntyre & Cullen, 2005) in continuous light at c. 190 $\mu\text{mol photons m}^2 \text{s}^{-1}$ at a temperature of $18 \pm 1^\circ\text{C}$. The cultures were grown in 40-mL volumes of *f/2* (Guillard, 1975)
210 or *L1* (Guillard & Hargraves, 1993) seawater medium, and diluted into fresh media in mid-exponential phase in a laminar flow hood. The seawater was collected, and tangential flow filtered at the National Research Council of Canada's Marine Institute at Ketch Harbour, NS. It was refiltered through a 0.2- μm capsule filter (Cytiva Whatman Polycap Disposable Capsules: 75TC) and nutrient-enriched in autoclaved glassware or in sterile cell culture plates.

215 Cultures were monitored daily via chlorophyll *a* fluorescence, measured with a Turner 10AU fluorometer (Turner Designs, USA) and a FIRE fluorometer following a 30-minute dark acclimation period. The fluorometers were blanked daily with culture medium, and the FIRE was also standardized with a solution of 100 $\mu\text{mol L}^{-1}$ rhodamine *b* in E-Pure water. The estimates were corrected for the sensitivity setting and the blank. Single-turnover induction and relaxation curves measured with the FIRE were fit with Fireworx software (Audrey Ciochetto, née Barnett, <http://sourceforge.net/projects/fireworx/>) to estimate
220 minimum (F_0), maximum (F_m), and variable fluorescence ($F_v = F_m - F_0$), the quantum yield of electron transport at PSII, F_v/F_m , the photosynthetic cross-section, σ (\AA^2), and the turnover time of the PQ pool, τ (ms).



Daily specific growth rates, μ (d^{-1}) were calculated from the change in fluorescence measured with the 10AU according to Equation 3 (Wood et al., 2005):

$$\mu = \frac{\ln(F_t/F_0)}{\Delta t}, \quad (3)$$

225 where F_t is the fluorescence (Arb.) at the end of the time interval, F_0 is the fluorescence at the beginning of the time interval, and Δt (d) is the length of the time interval. Cultures were assumed to be in balanced growth when the coefficient of variation (CV) for daily estimates of μ and the quantum yield of photosystem II (PSII) electron transport, F_v/F_m , were <10% over 10 generations (MacIntyre & Cullen, 2005). Experiments were initiated once a culture was in balanced growth.

4.2 Modified Serial Dilution Culture – Most Probable Number Assay

230 The concentration of viable cells following alkalization was estimated with the Serial Dilution Culture – Most Probable Number (SDC – MPN) assay (McCrary, 1915; Throndsen, 1978), using the methodology developed and validated by MacIntyre et al. (2018, 2019). The method was modified to use sterile 24-well polystyrene cell culture plates (Sigma Aldrich), based on the approach described by Bernd and Cook (2002), rather than individual tubes. The assays were set up with 8 replicates in each of 6 tiers of successive 10^{-1} dilutions. The dilutions were made with fresh sterile culture medium. The
235 concentrations of viable cells at the end of the grow-out period were estimated using an online calculator (EPA, USA; <https://mostprobablenumbercalculator.epa.gov/mpnForm>). These were expressed relative to the initial cell concentration, estimated using a hemocytometer with an inverted microscope (Leica Microsystems), as described by MacIntyre et al. (2018), as the Relative Viability (dimensionless).

240 The SDC–MPN incubations were set up by alkalizing 40-mL volumes of culture with increasing volumes of a 0.5-mol L^{-1} solution of NaOH in about 100- $\mu\text{mol L}^{-1}$ increments. These additions increased the initial concentration of total alkalinity, 2168 $\mu\text{mol L}^{-1}$, by 0–1084 $\mu\text{mol L}^{-1}$. The culture and NaOH were mixed and allowed to react for 10 minutes before dividing into two aliquots. The first was used for the serial dilutions. The second was used for measurement of T_0 fluorescence, F_v/F_m , and cell counts. These parameters were measured following set-up of the SDC-MPN assays, 1-2 hours after alkalization.

245

Following inoculation, the plates were placed on a light table illuminated from below with white LEDs at c. 190 $\mu\text{mol photons m}^{-2} \text{ s}^{-1}$ at a temperature of 18 ± 1 °C (i.e., the same conditions to which the cultures had been acclimated). To minimize the likelihood of desiccation or carbon limitation of growth, the plates were kept in sealed glass boxes containing an open 100-ml container of 1 mmol l^{-1} solution of sodium bicarbonate (NaHCO_3) to maintain high humidity. Chlorophyll
250 fluorescence was monitored daily with Synergy4 plate reader (BioTek, Winooski, VT, USA) after dark acclimation for 20 minutes. Following measurement, the plates were returned to the transparent boxes. Immediately before closure, 400 μL of 10% HCl was added to the NaHCO_3 reservoir to generate CO_2 , minimizing the likelihood of the cultures becoming carbon limited.



4.3 Chronic vs. transient exposure to elevated alkalinity

255 4.3.1 Response to chronic elevated alkalinity in *Thalassiosira pseudonana* and *Diacronema lutheri*

Cultures of *T. pseudonana* and *D. lutheri* were maintained in balanced, nutrient-replete growth as described in Section 4.1 to test for impacts from chronic exposure to elevated alkalinity and pH. Once in balanced growth, the cultures were transferred into fresh sterile media in a laminar flow hood under low light and treated with NaOH to increase the pH and alkalinity. Treatments consisted of additions of 100 – 1000 $\mu\text{mol L}^{-1}$ NaOH (final concentrations), yielding initial pH values of 8.13, 260 8.34, 8.57, 8.69, and 8.82. The treated cultures, and controls to which an equivalent volume of E-pure water had been added, were divided into two aliquots, one for measurement of pH and one for measurement of growth response. The latter were transferred into 6-mL sterile, borosilicate glass tubes in replicate, and kept in the dark until measurement of chlorophyll fluorescence (see Section 4.1). The culture tubes were grown into stationary phase, with fluorescence *in vivo* being measured daily to calculate the instantaneous and maximum growth rates using Equations 4a, 4b, and 5. Equation 4 is a modification of 265 Equation 1 that allows for a period of monitoring in which the signal does not change, either because the culture is in lag phase or because the signal is below the lower limit of detection.

$$\ln[F_t] = \ln[F_{init}] \text{ for } t \leq t_{lag} \quad (4a)$$

$$\ln[F_t] = (\ln[F_{fin}] - \ln[F_{init}]) \cdot \frac{t - t_{lag}}{((t_{exp})^b + (t - t_{lag})^b)^{\frac{1}{b}}} + \ln[F_{init}] \text{ for } t > t_{lag} \quad (4b)$$

$$\mu_m = \frac{\ln[F_{fin}] - \ln[F_{init}]}{t_{exp}} \quad (5)$$

270 where t is time (d); F_{init} , F_{fin} , and F_t are fluorescence (Arb.) at $t = 0$, in stationary phase, and at time t ; t_{lag} and t_{exp} are the durations of the lag and exponential phases of growth (d); and b (dimensionless) is a parameter that defines the curvature as the growth rate declines in the transition between exponential and stationary phase.

The average value of F_v/F_m at mid-exponential phase for each initial pH tested is shown in Figure 4a. Mid-exponential phase 275 was chosen because the cultures had been exposed to the elevated pH for approximately 2 days but were not yet experiencing nutrient limitation during stationary phase that would impact F_v/F_m (Kolber et al., 1998). The trends are not significant ($p > 0.05$), based on linear regression.

Variations in μ_m (Equation 5) in each treatment are illustrated in Figure 4b. The cultures were exposed to the elevated pH for 280 a period of 8 days in batch culture. The pH-dependence was calculated using Equations 2a & c with μ_m (rather than μ) as the dependent variable. In both cases, the fits were significant ($p < 0.05$). The threshold values of pH above which the exponential growth rates declined were 8.59 ± 0.06 for *T. pseudonana* and 8.68 ± 0.20 for *D. lutheri*. These thresholds align with the thresholds calculated from the literature in Section 2.3.

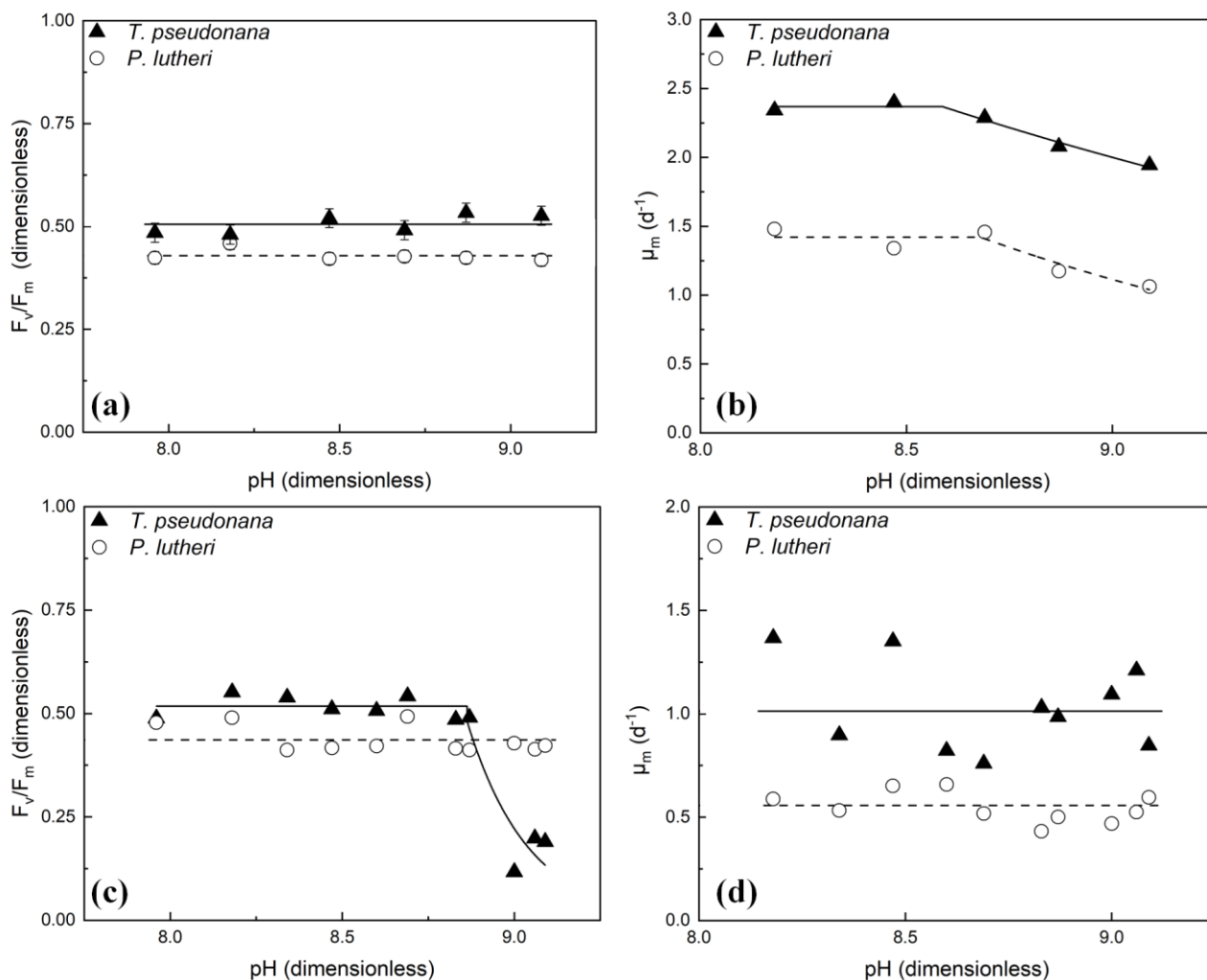


Figure 4: Variation in (a) F_v/F_m in mid-exponential phase and (b) μ_m during chronic exposure to elevated pH in *T. pseudonana* and *D. lutheri*. There was no significant trend in F_v/F_m for either species ($p > 0.05$). The fits to Equations 2 are shown in (b). Measurements of (c) the quantum yield of PSII electron transport, F_v/F_m , a measure of the proportion of functional reaction centres, and (d) the maximum fluorescence-based specific growth rate, μ_m , measured after exposure to elevated alkalinity and pH for 1-2 hours in *T. pseudonana* and *D. lutheri*. There was no significant trend in the data for F_v/F_m in *D. lutheri* nor for μ_m in either species. The dashed lines are the mean values. The reduction in F_v/F_m in *T. pseudonana* was fit to Equation 2 (dashed line). The estimated threshold pH for reduced F_v/F_m is 8.86 ± 0.24 .



285 **4.3.2 Response to transient elevated alkalinity**

The effect of 10-minute exposure to elevated alkalinity and pH on viability in *T. pseudonana* and *D. lutheri* are illustrated in Figure 5. In both cases, there is no evidence for an effect of transient exposure to high alkalinity on viability: Type 1 regressions of RV on pH were not significant ($p > 0.05$). Even with high replication and multiple tiers of dilution, the 95% confidence intervals span about an order of magnitude. In all samples, RV of 1 — the value at which the concentration of viable cells is equal to the total cell concentration — is within the 95% CI of the estimate.

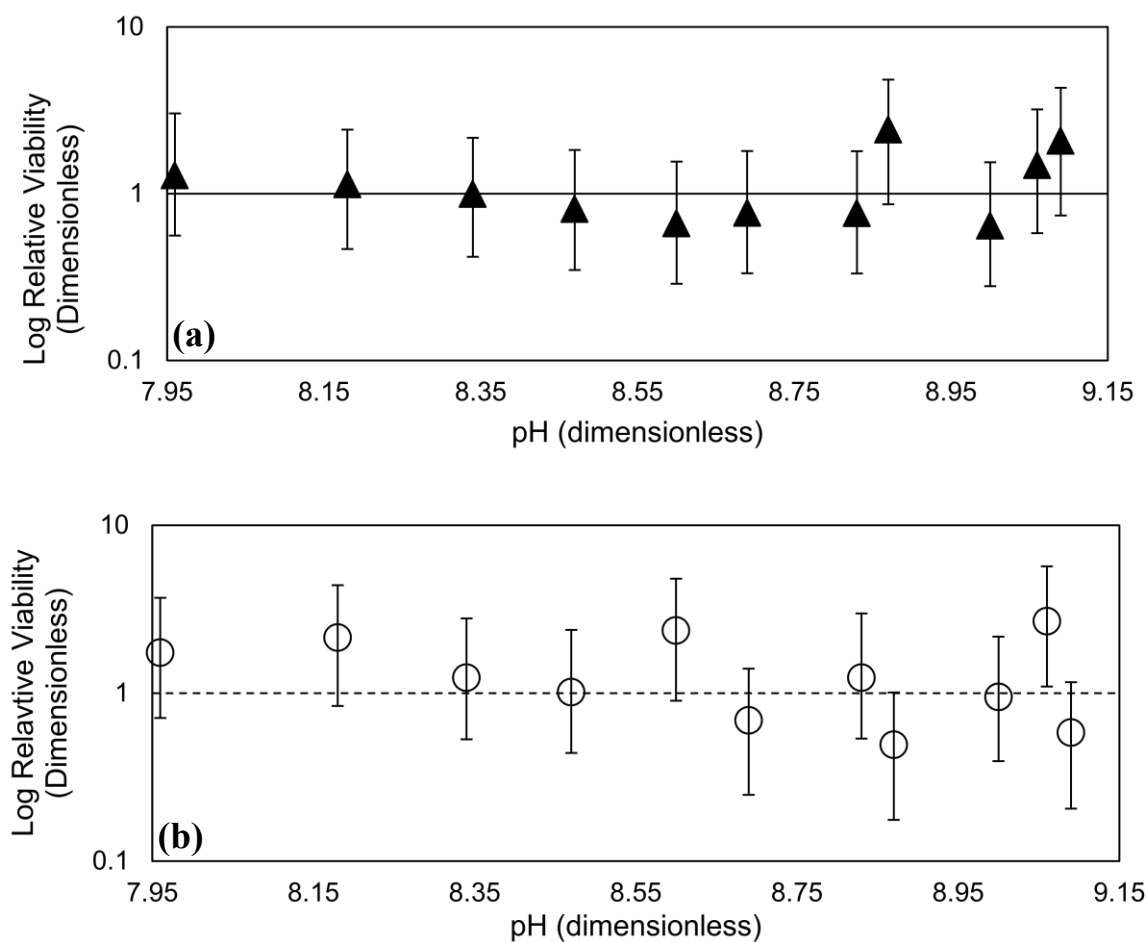


Figure 5: Dose-response curves showing the effect of transient exposure to increasing alkalinity pH on RV of a) *T. pseudonana* and b) *D. lutheri*. Error bars are the 95% CI, and the dashed line is a RV of 1 (*i.e.*, no change). Regressions of RV on pH were not significant ($p > 0.05$).



The effects of transient alkalization on the proportion of functional PSII reaction centres, F_v/F_m , and the maximum specific growth rate, μ_m , were examined with the same methods as the chronic exposure. The average value F_v/F_m for *D. lutheri* was 295 0.43, indistinguishable from the values in the untreated parent culture, and there was no significant trend ($p>0.05$) with the transient elevation in pH (Figure 4c). There was a significant trend for *T. pseudonana* (Figure 4c). The data were fit with the biphasic model (Equation 2) and the threshold pH at which there was a reduction was estimated as 8.86 ± 0.24 .

The 10^{-3} dilution from the SDC – MPN assays was used to calculate μ_m , the maximum (exponential phase) growth rate, for 300 each treatment because it was the lower dilution common to all treatments. Note that at a 10^{-3} dilution, even the highest hydroxide addition would have been diluted back to background concentrations, so these samples were growing in the original seawater medium. There was no discernible impact of transient exposure to high alkalinity on μ_m in either species (Figure 4d). Neither a linear regression nor the bilinear model (Equation 2) gave statistically significant fits to the data ($p>0.05$).

5 Discussion and Conclusions

305 The immediate outcome of OAE in surface waters will be an increase in alkalinity and pH. Public acceptance of the approach to CDR will hinge on both measurement, reporting and verification of carbon capture, which is beyond the scope of this study, and on potential impacts on the ocean. The synthesis of studies from the literature suggests that significant long-term increases in pH to 8.2–8.3 would not affect the growth rates of the majority of species studied. However, the conclusion needs to be qualified in the context of OAE, as the experiments were conducted in pH-drift cultures in which CO_2 replacement is prevented. 310 The mechanism of OAE turns on CO_2 invasion to restore the equilibrium concentration of CO_2 after conversion of existing CO_2 to bicarbonate. Comparisons of alkalized cultures with high DIC (semi-continuous cultures or aerated batch cultures) and those in which there was a drawdown (sealed pH drift cultures) show that in some cases there is no difference in the resulting growth rates (the dinoflagellates *Ceratium furca* and *C. fusus*; Figure 2) but in others it is pronounced (the dinoflagellate *C. tripos* and the diatom *Thalassiosira pseudonana*; Figures 2 and 3). This suggests that evaluation of OAE in the context of the 315 pH-drift cultures should be done with caution.

The analysis of prior studies of pH-dependant growth rates indicates that dinoflagellates are statistical outliers among the taxonomic groups and may be more sensitive to alkalization than most others. This might be because there is more complete sampling of this group than of the others. They were the primary focus for these researchers' studies, which were prompted by 320 the observation that dinoflagellates dominated the summer assemblages in nearby Mariager Fjord when pH is most likely to be high (Hansen, 2002; Hansen et al., 2007; Berge et al., 2010; Berge et al., 2012; Søderberg & Hansen, 2007). Their higher sensitivity to raised pH might also reflect fundamental differences in the dinoflagellates' physiology and ecology. Rost et al. (2006) investigated 3 species of dinoflagellates, some tested in the pH-drift studies, demonstrated that they had robust CCMs that were dominated by bicarbonate rather than CO_2 transport, even at high pH (8.5–9.1), and concluded that the CCM was



325 unlikely to be limiting to growth. This suggests that their higher sensitivity to alkalization is not related to photosynthetic
carbon uptake, in spite of the low CO₂ affinity of the L2 isoform of Rubisco (Iñiguez et al., 2020) found in peridinin-containing
dinoflagellates. Their dominance at times when their sensitivity to pH suggests they should be the most impacted might be
attributed to their frequent use of mixotrophy (reviewed by Stoecker et al., 2017), the combination of photosynthesis and
feeding rather than photosynthesis alone, a trait that confers an advantage for nutrient acquisition during stratification events
330 (Margalef, 1978). There was no indication that the dinoflagellate cultures were fed during the pH-drift experiments. If so, the
increased sensitivity might not affect growth in natural environments where feeding is possible. In short, the apparent
sensitivity of dinoflagellates to elevated pH should not be extrapolated to natural assemblages subjected to OAE without further
study of its effect on feeding and mixotrophic growth.

335 A last reason for caution in extrapolating the pH-drift responses lies with the most probably scenario for conducting OAE,
discharge in the nearshore (to avoid contravention of the London Convention), likely into strong lateral flow. Under these
conditions, exposure to elevated pH would be relatively short until such time as cumulative discharge of alkalinity raised the
pH of the entire water body. The combination of dilution by transport and reaction of the alkalinity with CO₂ (followed by
CO₂ invasion) would greatly reduce the timescale of exposure to elevated pH. With this in mind, we conducted experiments
340 to compare the response of *Thalassiosira pseudonana* and *Diacronema lutheri* to chronic (longer than 5 hours) and transient
(10-minutes) exposure to elevated pH and alkalinity. There were reductions in growth rate at high pH in both.

The threshold values for reductions in growth rate with chronic exposure were 8.59 and 8.68 for *T. pseudonana* and *D. lutheri*,
respectively. These align with the average threshold values observed in Figure 1d for diatoms (8.23 – 9.56) and
345 prymnesiophytes (8.47 – 8.69) measured in pH-drift experiments, as expected from the fact that they were performed under
comparable conditions (sealed cultures with minimal headspace for gas exchange). Although growth rates were reduced, there
was no evidence of a reduction in photosynthetic efficiency, as inferred from F_v/F_m measured in the midpoint of exponential
phase growth, indicating that the growth-limiting step was downstream of light harvesting and charge separation in PSII.

350 Transient exposure to elevated pH did not have a statistically significant impact on F_v/F_m for *D. lutheri*, however there was a
significant reduction in *T. pseudonana* at the highest pH values tested (8.87 – 9.09). The lack of an effect under chronic
exposure to elevated pH in the same species suggests that it takes between 2 hours and several days for recovery (photorepair)
of *T. pseudonana* acclimated to elevated pH. There was no evidence for persistent reductions in growth rate, nor viability,
measured in the days following transient exposure. We note that at the pH in our experiments, the dominant carbon species
355 would be carbonate and calcite would begin precipitating; the reductions in bicarbonate available for the CCM might account
for the reductions in growth rates observed in Figure 4. Elevating the pH this high is highly undesirable from the perspective
of OAE, as calcite precipitation releases CO₂ rather than traps it. It would be possible through the accidental discharge of a



concentrated hydroxide slurry, though, so the degree of impairment represents a worst-case scenario rather than the response under expected discharge conditions.

360

The transient exposures were conducted with only two species, so cannot be considered representative of phytoplankton in general. However, they show clearly that there are significant differences between the effects of transient and long-term exposure to elevated pH. There are significant changes in growth rates with chronic exposure to elevated pH that are consistent with reports from the literature but are not observed following transient exposure to the same range of high pH. If consistent results are found across taxa or in mixed assemblages, the estimates of threshold pH at which growth rates were reduced — which were all based on chronic exposure in pH-drift or semi-continuous culture, — are likely to overestimate the potential impact of OAE if the alkalinity is diluted on timescales of 10 minutes to 1-2 hours following discharge into the receiving waters.

365

370 *Data Availability*

Data will be made available upon request.

Author Contributions

JLO and HLM designed the experiments and JLO, MB, and CL conducted them. HLM supervised the study. JLO was responsible for the literature review, data digitization, data analysis, and statistical analysis. JLO and HLM prepared the manuscript.

375

Competing Interests

The contact author has declared that none of the authors have any competing interests.

380

Acknowledgements

This research was funded through the ClimateWorks Foundation and the Thistledown Foundation donations, and the Natural Sciences and Engineering Research Council of Canada grant CRDPJ 520352-17. The authors would like to thank Mikeala Ermanovics and Rose Latimer for assistance with conducting experiments and culture maintenance.

385 References

Badger, M. R., Andrews, T. J., Whitney, S. M., Ludwig, M., Yellowless, D. C., Leggat, W., and Price, G. D.: The diversity and coevolution of Rubisco, plastids, pyrenoids, and chloroplast-based CO₂-concentrating mechanisms in algae, *Can. J. Botany*, 76(6), 1052-1071, doi:10.1139/b98-074, 1998.



- Badger, M. R. and Bek, E. J.: Multiple Rubisco forms in proteobacteria: their functional significance in relation to CO₂ acquisition by the CBB cycle, *J. Exp. Bot.*, 59, 1525–1541, doi:10.1093/jxb/erm297, 2008.
- 390 Berge, T., Daugbjerg, N., and Hansen, P. J.: Effect if lowered pH on marine phytoplankton growth rates, *Mar. Ecol. Prog. Ser.*, 416, 79–91, doi:10.3354/meps08780, 2010.
- Bannister, T. T.: Quantitative description of steady state, nutrient-saturated algal growth, including adaptation, *Limnol. Oceanogr.*, 24, 76-96, 1979.
- 395 Berge, T., Daugbjerg, N., and Hansen, P. J.: Isolation and cultivation of microalgae select for low growth rate and tolerance to high pH, *Harmful Algae*, 20, 101–110, doi:10.1016/j.hal.2012.08.006, 2012.
- Bernd, K. K. and Cook, N.: Microscale Assay Monitors Algal Growth Characteristics, *BioTechniques*, 32, 1256-1259, 2002.
- Colman B., Huertas, I. E., Bhatti, S., and Dason, J. S.: The diversity of inorganic carbon acquisition mechanisms in eukaryotic microalgae, *Funct. Plant Biol.*, 29(3), 261, doi: 10.1071/PP01184, 2002.
- 400 Galland, G., Harrould-Kolieb, E., and Herr, D.: The ocean and climate change policy, *Climate Policy*, 12(6), 764-771, doi:0.1080/14693062.2012.692207, 2012.
- Guillard, R. R. L.: Culture of phytoplankton for feeding marine invertebrates, in: *Culture of marine invertebrate animals*, edited by: Smith, W. L., and Chanley, M. H., Plenum, New York, 108-132, doi:10.1007/978-1-4615-8714-9_3, 1975.
- Guillard, R. R. L., and Hargraves, P. E.: *Stichochrysis immobilis* is a diatom, not a chrysophyte, *Phycologia*, 32, 234-236, doi: 10.2216/i0031-8884-32-3-234.1, 1993.
- 405 Hansen, P. J.: Effect of high pH on the growth and survival of marine phytoplankton: Implications for species succession, *Aquat. Microb. Ecol.*, 28, 179-288, doi:10.3354/ame028279, 2002.
- Hansen, P. J., Lundholm, N., and Rost, B.: Growth limitation in marine red-tide dinoflagellates: Effects of pH versus inorganic carbon availability, *Mar Ecol Prog Ser*, 334, 63–71, doi:10.3354/meps334063, 2007.
- 410 Hijnen, W. A. M, Beerendonk, E. F., and Medema, G. J.: Inactivation credit of UV radiation for viruses, bacteria and protozoan (oo)cysts in water: A review, *Water Res*, 40, 3-22, doi:10.1016/j.watres.2005.10.030, 2006.
- Iñiguez, C., Capó-Bauçà, S., Niinements, Ü., Stoll, H., Aguiló-Nicolau, P., Galmés, J.: Evolutionary trends in RuBisCO kinetics and their co-evolution with CO₂ concentrating mechanisms, *Plant J.*, 101(4), 897-918, doi:10.1111/tpj.14643, 2020.
- Jordan, D. B. and Ogren, W. L.: Species variation in the specificity of ribulose biphosphate carboxylase/oxygenase, *Nature*, 415 291, 513-515, doi:10.1038/291513a0, 1981.
- Jones, C. T., Craig, S. E., Barnett, A. B., MacIntyre, H. L., Cullen, J. J.: Curvature in models of the photosynthesis-irradiance response, *J. Phycol.*, 50(2), 341-355, doi:10.1111/jpy.12164, 2014.
- Kolber, Z., Zehr, J., Falkowski, P.: Effects of growth irradiance and nitrogen limitation on photosynthetic energy conversion in photosystem II, *Plant Physiol.*, 88, 923-929, doi: 10.1104/pp.88.3.923, 1998.
- 420 Lenton, A., Matear, R. J., Keller, D. P., Scott, V., and Vaughan, N. E.: Assessing carbon dioxide removal through global and regional ocean alkalization under high and low carbon emission pathways, *Earth Syst. Dyn.*, 9(2), 339-359, doi:10.5194/esd-9-339-2018, 2018.



- Lewis, E., and Wallace, D.: Program developed for CO₂ system calculations, Carbon Dioxide Information Analysis Center, managed by Lockheed Martin Energy Research Corporation for the US Department of Energy Tennessee, 1998.
- 425 Li, W. K. W., and Dickie, P. M.: Monitoring phytoplankton, bacterioplankton, and virioplankton in a coastal inlet (Bedford Basin) by flow cytometry, *Cytometry*, 44(3), 236-246, doi: 10.1002/1097-0320(20010701)44:3<236::aid-cyto1116>3.0.co;2-5, 2001.
- Li, W. K. W., and Harrison, G. W.: Propagation of an atmospheric climate signal to phytoplankton in a small marine basin, *Limnol. Oceanogr.*, 53(3), 1734-1745, doi: 10.4319/lo.2008.53.5.1734, 2008.
- 430 MacIntyre, H. L., and Cullen, J. J.: Using Cultures to Investigate the Physiological Ecology of Microalgae, in: *Algal Culturing Techniques*, edited by: Andersen, R. A., Academic Press, 287-326, doi:10.1016/B978-012088426-1/50020-2, 2005.
- MacIntyre H. L., Cullen, J. J., Whitsitt, T. J., and Petri, B.: Enumerating viable phytoplankton using a culture-based Most Probable Number assay following ultraviolet-C treatment, *J Appl Phycol*, 30, 1073–1094, doi:10.1007/s10811-017-1254-8, 2018.
- 435 MacIntyre, H. L., Cullen, J. J., Rastin, S., Waclawik, M., Franklin, K. J., Poulton, N., Lubelczyk, L., McPhee, K., Richardson, T. L., Van Meerssche, E., Petri, B.: Inter-laboratory validation of the serial dilution culture-most probable number method for enumerating viable phytoplankton, *J. Appl. Phycol.*, 31(1), 491-503, doi:10.1007/s10811-018-1541-z, 2019.
- Margalef, R.: Life-forms of phytoplankton as survival alternatives in an unstable environment, *Oceanol Acta*, 1, 493-509, 1978.
- 440 McCrady, M. H.: The numerical interpretation of fermentation-tube results, *J. Infect. Dis.*, 17(1), 183-212, 1915.
- Nielsen, L. T., Lundholm, N., and Hansen, P. J.: Does irradiance influence the tolerance of marine phytoplankton to high pH? *Mar Bio Res*, 3(6), 446-453, doi:10.1080/17451000701711820, 2007.
- Nimer, N. A., Iglesias-Rodriguez M. D., and Merrett, M. J.: Bicarbonate utilization by marine phytoplankton species, *J. Phycol.*, 33, 625-631, doi:10.1111/j.0022-3646.1997.00625.x, 1997.
- 445 Raven, J. A., Beardall, J., and Giordano, M.: Energy costs of carbon dioxide concentrating mechanisms in aquatic organisms, *Photosynth. Res.*, 121(2-3), 111-124, doi: 10.1007/s11120-013-9962-7, 2014.
- Raven, J. A., Beardall, J., and Sánchez-Baracaldo P.: The possible evolution and future of CO₂-concentrating mechanisms. *J. Exp. Bot.*, 68(14), 3701-3716, doi:10.1093/jxb/erx110, 2017.
- Renforth, P. and Henderson, G.: Assessing ocean alkalinity for carbon sequestration: Ocean alkalinity for C sequestration, 450 *Rev. Geophys.*, 55(3), 636-674, doi:10.1002/2016RG000533, 2017.
- Rost, B., Richter, K.-U., Riebesell, U., and Hansen, P. J.: Inorganic carbon acquisition in red tide dinoflagellates, *Plant, Cell & Environment*, 29(5), 810-822, doi.org/10.1111/j.1365-3040.2005.01450.x, 2006.
- Shih, P. M., Occhialini, A., Cameron, J. C., Andralojc, P. J., Parry, M. A., and Kerfeld, C. A.: Biochemical characterization of predicted Precambrian RuBisCO, *Nat. Commun.* 7, doi:10.1038/ncomms10382, 2016.
- 455 Söderberg, L., and Hansen, P.: Growth limitation due to high pH and low inorganic carbon concentrations in temperate species of the dinoflagellate genus *Ceratium*, *Mar Ecol Prog Ser*, 351, 103–112, doi:10.3354/meps07146, 2007.



- Søgaard, D.H., Hansen, P.J., Rysgaard, S., and Glud, R.N.: Growth limitation of three Arctic sea ice algal species: Effects of salinity, pH, and inorganic carbon availability, *Polar Biology*, 34(8), 1157–1165, doi:10.1007/s00300-011-0976-3, 2011.
- Stoecker, D.K.: Mixotrophy among Dinoflagellates. *J Eukaryot Microbiol*, 46(4), 397–401, doi:10.1111/j.1550-4607408.1999.tb04619.x, 1999.
- Stoecker, D. K., Hansen, P. J., Caron, D. A., Mitra, A.: Mixotrophy in the marine plankton, In: *Annual Review of Marine Sciences*, 9, 311-335. doi:10.1146/annurev-marine-010816-060617, 2017.
- Tcherkez, G. G. B., Farquhar, G. D., and Andrews, T. J.: Despite slow catalysis and confused substrate specificities, all ribulose biphosphate carboxylases may be nearly perfectly optimized, *Proc. Natl. Acad. Sci. U.S.A.*, 103, 7246-7251, doi:10.1073/pnas.0600605103, 2006.
- Thronsdén, J.: The dilution-culture method, In: Sournia A (ed) *Phytoplankton Manual*, UNSECO, Paris, 218-224, 1978.
- Weavers, L.K., and Wickramanayake, G.B.: Kinetics of the inactivation of microorganisms, In: Block SS (ed) *Disinfection, Sterilization, and Preservation*, 5th ed. Lippincott Williams & Wilkins, Philadelphia, PA, pp 65-78.
- Whitney, S. M., Andrews, T. J.: The CO₂/O₂ specificity of single-subunit ribulose-bisphosphate carboxylase from the dinoflagellate, *Amphidinium carterae*, *Aust. J. Plant. Physiol.*, 25, 131-138, 1998.
- Winder, M., and Sommer, U.: Phytoplankton response to a changing climate, *Hydrobiologia*, 689(1), 5-16, doi:10.1007/s10750-012-1149-2, 2012.
- Wood, M. A., Everroad, R. C., Wingard, L. M.: Measuring growth rates in microalgal cultures, in: *Algal Culture Techniques*, edited by: Andersen, R. A., 269-285, doi:10.1016/B978-012088426-1/50020-2, 2005.
- Zwietering, M. H., Jongenburger, I., Rombouts, F. M., Vantriet, K.: Modeling of the bacterial growth curve, *Appl. Environ. Microbiol.*, 56(6), 1875-1881, 1990.